Configuration and Control for AC-DC Three Degrees of Freedom Hybrid Magnetic Bearings *

Huangqiu Zhu, Huaixiang Chen, Zhiyi Xie, and Yang Zhou
School of Electrical and Information Engineering
Jiangsu University
Xuefu Road 301, 212013 Zhenjiang, China
zhuhuangqiu@ujs.edu.cn

***Abstract* – In this paper, an innovated AC-DC 3 degrees of freedom hybrid magnetic bearing is proposed, which is driven by a DC amplifier in axial direction and a 3-phase power converter in radial directions respectively, and the axial and radial bias magnetic fluxes are provided by a common radial polarized permanent magnet ring. The principle of producing magnetic suspension forces is introduced. By using equivalent magnetic circuit method, the calculation formulas of magnetic suspension forces and the mathematics models of the system are deduced. Nonlinearities of suspension forces and cross coupling between different degrees of freedom are studied further by calculating the suspension forces at different displacements and control currents to validate the feasibility of the mathematics models. Then based on the mathematics models of the bearing, a digital control method of this novel bearing is designed. The theory analysis and test results have shown that this magnetic bearing incorporates the merits of 3-phase AC drive, permanent magnet flux biased and axial-radial combined control, and reduces overall system size and has higher efficiency and lower cost.**

***Index Terms* – Hybrid magnetic bearing, Equivalent flux path, Mathematics model, Nonlinearity, Finite element analysis.**

I. INTRODUCTION

Magnetic bearings can be classified as axial single degree of freedom, radial 2 degrees of freedom and axial-radial 3 degrees of freedom by its restriction function. A 3 degrees of freedom magnetic bearing integrates an axial bearing and a radial bearing into a whole one, so the configuration of this bearing is simplified and the overall size is reduced. According to principle of producing suspension forces, magnetic bearings can be classified as passive magnetic bearing, active magnetic bearing and hybrid magnetic bearing. Hybrid magnetic bearing depends on a permanent magnet to provide the bias flux and several electromagnetic coils to supply the control fluxes, so the volume of its power amplifier is much smaller than active magnetic bearing, and this kind of bearing has a compact structure and lower power consumption, meanwhile, larger air gap can be realized due to the permanent magnet biased. Furthermore, based on the exciting current types, magnetic bearings can be classified as DC magnetic bearing and AC magnetic bearing. A radial magnetic bearing is usually operated with four channel power amplifiers, and the cost of DC power amplifier is high. However, an AC magnetic bearing can be driven by an industrial 3-phase converter. 3-phase converters are used in huge quantities for electrical drives and are available at very low prices, they can be incorporated with high performance digital signal processor, which makes it very easy to rewrite or update the software of the controller in a magnetic bearing system. At present, DC 3 degrees of freedom HMBs have been designed [1]-[2]; AC 2 degrees of freedom HMBs have been designed too and applied in the bearingless canned motor pump in Switzerland [3]. The AC-DC 3 degrees of freedom hybrid magnetic bearing incorporates the merits of AC exciting, permanent magnet flux biased and axial-radial combined control, so this magnetic bearing has many applications in super-speed and super-precision numerical control machine tools, bearingless motors, high-speed flywheels, satellites, etc.

II. CONFIGURATION AND PRINCIPLE

A. Configuration of AC-DC 3 Degrees of Freedom HMB

Fig.1 shows the configuration of AC-DC 3 degrees of freedom HMB, which consists of an axial stator, two axial control coils, a radial stator with three poles, three radial control coils, a rotor and a permanent magnet ring magnetized radially, etc. The flux generated by both of the axial control coils is used to control the axial single degree of freedom, and the resultant flux generated by three radial coils arranged around the rotor is used to control the radial 2 degrees of freedom. Radial stator is made of stacked iron sheets; the permanent magnet material is Neodymium-iron-boron. If there is no external disturbance or load, the static attracting forces generated by the permanent magnet will levitate the rotor in the ideal balance position. Both the radial and the axial air-gap length are taken as 0.5 mm.

B. Principle of AC-DC 3 Degrees of Freedom HMB

The magnetic flux path of AC-DC 3 degrees of freedom HMB is presented in Fig.2. In Fig.2, *A*, *B* and *C* represents each pole's position respectively, i_z is the axial control

* This work is supported by National Natural Science Foundation of China (NSFC)(50575099).

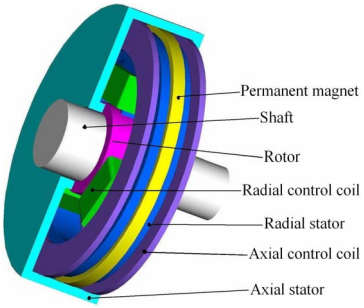

Fig.1 Assembling structure of AC-DC 3 degrees of freedom HMB

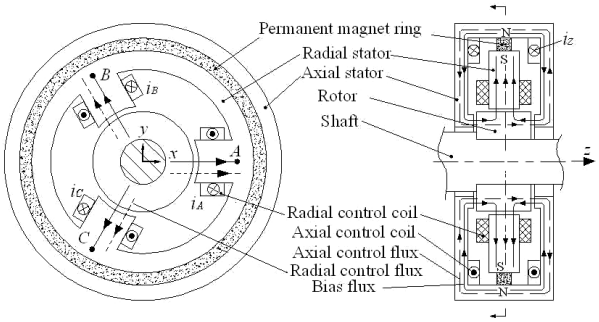

Fig.2 Configuration of AC-DC 3 degrees of freedom HMB

current, i_A, i_B and i_C are the radial control currents respectively. The real lines with arrows represent the static bias flux generated by the permanent magnet, which start from N-pole of the permanent magnet, flow through the axial stator, the axial air gap, the rotor, the radial air gap, then come back through the radial stator to S-pole of the permanent magnet. The dashed lines with arrows (the arrow direction of the control magnetic flux is determined by the control current direction in right hand rule) represent the control fluxes generated by the control coils, the axial control flux is conducted by the axial stator, axial air gap and the rotor; the radial control flux is conducted by the radial stator, radial air gap and the rotor. As shown in the sketch Fig.2, the axial flux and the radial flux do not influence each other, so the coupling between them is very little. The static biased flux and the control flux are superimposed or subtracted in each air gap.

The flux quantities of permanent biased magnetic fluxes are the same in both of the axial air gaps when the rotor is in the axial reference balance position. If the rotor is displaced in the axial direction by a disturbance force, the axial permanent flux will be increased and the magnetic force will be increased correspondingly in the reduced air gap. Whereas the other axial permanent flux will be reduced in the increased air gap, the magnetic force will be decreased. As long as the control flux is content with the following expression

$$\phi_{cz} \geq \frac{\phi_{pz1} - \phi_{pz2}}{2} \tag{1}$$

where ϕ_{cz} —— Axial control flux

ϕ_{pz1} —— Axial permanent flux in reduced axial air gap

ϕ_{pz2} —— Axial permanent flux in increased axial air gap

Then no matter a left or right external disturbance is applied to the rotor, the axial control system with a negative position feedback will adjust the exciting current of the axial control coils to control the flux of the air gap, and levitate the rotor in the ideal axial balance position.

Based on principle of bearingless motor, superposing an additional bearing windings flux distribution with pole pair number $p_2 = p_1 \pm 1$, p_1 is the pole pair number of motor windings. Maxwell lateral forces can be set up and be used to support the rotor without contact [4]. If p_1=0, p_2=1, the bearingless motor is changed to be a radial magnetic bearing with radial suspension force in fact. Based on motor theories, applied 3-phase AC to the radial three control coils arranged around the rotor symmetrically, the exciting current would generate a rotated magnetic field and form a unipolar incorporated magnetic flux. When the rotor is displaced from the balance position due to radial disturbances, the radial position sensors measure the position of the rotor and transfer the position signals to the controller, the controller calculates the displacements of x and y and transforms them into control current signals, the power amplifier is driven by the control signals and outputs exciting currents, in this way, the exciting currents generate control fluxes, which is superposed with the biased flux, then a flux increase can be created in half the bearing and a flux decrease in the other half, so adjusting exciting currents, the resulting force can be pointed in any direction and levitate the rotor in the ideal radial position.

III. MATHEMATICS MODELS

A. Calculation of the Equivalent Magnetic Flux Path

To simplify calculation of the magnetic flux path, there are some assumptions on the flux path. Only the leakage of the inner and outer annulus of the permanent magnet are considered, the whole flux path system is taken as a parallel connection system composed by leakage reluctance and available fluxes; and as well, only the air gap reluctance is considered, the reluctance of the irons and the rotor and the eddy current losses are neglected. Therefore, the equivalent permanent magnet circuit is laid out in Fig.3.

In Fig.3, F_m is the magnetomotive force that the permanent magnet provides to the outer circuit, ϕ_m is the total magnetic flux that the permanent magnet generates,

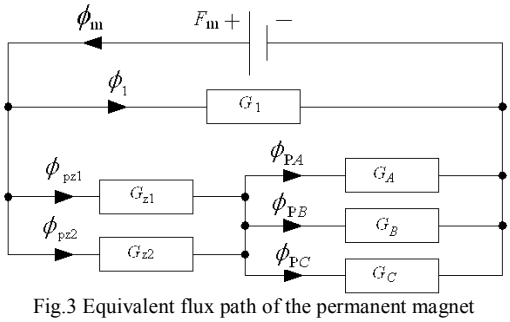

Fig.3 Equivalent flux path of the permanent magnet

ϕ_1 is the total magnetic flux leakage of the permanent magnet, the leakage permeance is G_l, G_{z1} and G_{z2} describe the positive and the negative air gap permeance respectively, and the radial air gap permeances are G_A, G_B and G_C respectively. Supposing that the rotor has a right displacement z in the axial direction and has positive displacements x and y in the two directions x and y respectively, then the magnetic permeance of each air gap can be calculated as follows

$$\begin{cases} G_{z1}=\dfrac{\mu_0 S_{\mathrm{a}}}{\delta_{\mathrm{a}}-z} \quad G_{z2}=\dfrac{\mu_0 S_{\mathrm{a}}}{\delta_{\mathrm{a}}+z} \\ G_A=\dfrac{\mu_0 S_{\mathrm{r}}}{\delta_{\mathrm{r}}-x} \\ G_B=\dfrac{\mu_0 S_{\mathrm{r}}}{\delta_{\mathrm{r}}+0.5x-\sqrt{3}y/2} \\ G_C=\dfrac{\mu_0 S_r}{\delta_{\mathrm{r}}+0.5x+\sqrt{3}y/2} \end{cases} \tag{2}$$

where μ_0 —— Permeability of the vacuum
S_{a} —— Axial magnetic pole area
S_{r} —— Radial magnetic pole area
δ_{a} —— Axial air gap length
δ_{r} —— Radial air gap length

Based on the Kirchhoff's laws of the magnetic circuit, the biased flux of each air gap in Fig.2 can be calculated as follows

$$\begin{cases} \phi_{\mathrm{pz}i}=\dfrac{(G_A+G_B+G_C)}{(G_{z1}+G_{z2})+(G_A+G_B+G_C)}F_{\mathrm{m}}G_{zi} \\ \phi_{\mathrm{pj}}=\dfrac{(G_{z1}+G_{z2})}{(G_{z1}+G_{z2})+(G_A+G_B+G_C)}F_{\mathrm{m}}G_j \end{cases} \tag{3}$$

where $i = 1, 2, j = A, B, C$

As can be seen from Fig.2, the biased and control flux superimpose additively or subtract in air gap, so the resultant magnetic flux of each air gap can be calculated as follows

$$\begin{cases} \phi_{z1}=\phi_{cz}-\phi_{\mathrm{pz}1}=N_z i_z G_{z1}-\phi_{\mathrm{pz}1} \\ \phi_{z2}=\phi_{cz}+\phi_{\mathrm{pz}2}=N_z i_z G_{z2}+\phi_{\mathrm{pz}2} \\ \phi_j=\phi_{cj}+\phi_{\mathrm{pj}}=N_r i_j G_j+\phi_{\mathrm{pj}} \end{cases} \tag{4}$$

where N_z —— Turns of the axial control coil
i_z —— Axial control current
N_{r} —— Turns of each radial control coil
i_j —— Radial control current
$j = A, B, C$

B. Expression on Axial Magnetic Attractive Force

If the rotor has a small displacement z to the right in axial direction, so a left resulting force is needed to make the rotor go back to the balance position. Based on the relationship between the magnetic force and the magnetic flux, the magnetic attractive force can be calculated as follows

$$F_z = F_{z2} - F_{z1} = \frac{\phi_{z2}^2-\phi_{z1}^2}{2\mu_0 S_{\mathrm{a}}} \tag{5}$$

where F_{z2} —— Left magnetic attractive force acted on the rotor

F_{z1} —— Right magnetic attractive force acted on the rotor

Substituting Eqs.(2), (3), (4) into Eq.(5), linearizing it and neglecting the dimensionless of over two rank at the balance position (x, y is much smaller than δ_{r}, z is much smaller than δ_{a}) lead to the following expression

$$F_z \approx \left.\frac{\partial F_z}{\partial z}\right|_{\substack{i_z=0\\x=y=z=0}} z+\left.\frac{\partial F_z}{\partial i_z}\right|_{\substack{i_z=0\\x=y=z=0}} i_z = k_z z + k_{iz} i_z \tag{6}$$

where
$$\begin{cases} k_z=-\dfrac{\mu_0 F_{\mathrm{m}}^2}{2\left(\dfrac{\delta_{\mathrm{a}}}{2S_{\mathrm{a}}}+\dfrac{\delta_{\mathrm{r}}}{3S_{\mathrm{r}}}\right)^2\delta_{\mathrm{a}}S_{\mathrm{a}}} \\ k_{iz}=\dfrac{\mu_0 F_{\mathrm{m}} N_z}{\left(\dfrac{\delta_{\mathrm{a}}}{2S_{\mathrm{a}}}+\dfrac{\delta_{\mathrm{r}}}{3S_{\mathrm{r}}}\right)\delta_{\mathrm{a}}} \end{cases}$$

k_z is called as axial force-displacement coefficient, k_{iz} is called as axial force-current coefficient. Both k_z and k_{iz} are constants after the configuration of the magnetic bearing and the balance position of the rotor is determined.

C. Expressions of Radial Magnetic Attractive Forces

Assuming that the rotor has positive displacements x and y in x- and y-direction respectively, then the magnetic attractive forces generated by the resulting magnetic flux of each radial air gap can be expressed as the follow

$$F_j = \frac{\phi_j^2}{2\mu_0 S_{\mathrm{r}}} \tag{7}$$

where $j=A, B, C$

Substituting Eqs.(2), (3), (4) into Eq.(7), under the assumption that the rotor has a very small displacement from the radial balance position, Eq.(7) can be linearized as the follow

$$F_j = F_j\left|_{\substack{i_j=0\\x=y=z=0}}+\left.\frac{\partial F_j}{\partial i_j}\right|_{\substack{i_j=0\\x=y=z=0}} i_j = F_{\mathrm{pm}}+k_{ir}\cdot i_j \right. \tag{8}$$

where
$$\begin{cases} F_{\mathrm{pm}}=\dfrac{\mu_0 F_{\mathrm{m}}^2}{18(\dfrac{\delta_{\mathrm{a}}}{2S_{\mathrm{a}}}+\dfrac{\delta_{\mathrm{r}}}{3S_{\mathrm{r}}})^2 S_{\mathrm{r}}} \\ k_{ir}=\dfrac{\mu_0 F_{\mathrm{m}} N_r}{3(\dfrac{\delta_{\mathrm{a}}}{2S_{\mathrm{a}}}+\dfrac{\delta_{\mathrm{r}}}{3S_{\mathrm{r}}})\delta_{\mathrm{r}}} \end{cases}$$

$j=A, B, C$

F_{pm} is the magnetomotive force generated by the permanent magnet flux in each radial air gap, whose value is the same in each radial air gap when the rotor is in the balance position, k_{ir} is called as radial force-current coefficient, Both F_{pm} and k_{ir} are constants after the

configuration of the magnetic bearing and the balance position of the rotor is determined.

The resulting forces in x- and y-direction can be calculated as follows

$$F_x = F_A - \frac{1}{2}F_B - \frac{1}{2}F_C = k_{ir}i_A - \frac{1}{2}k_{ir}i_B - \frac{1}{2}k_{ir}i_C \quad (9)$$

$$F_y = \frac{\sqrt{3}}{2}F_B - \frac{\sqrt{3}}{2}F_C = \frac{\sqrt{3}}{2}k_{ir}i_B - \frac{\sqrt{3}}{2}k_{ir}i_C \quad (10)$$

The condition for a 3-phase system is applicable

$$i_A + i_B + i_C = 0 \quad (11)$$

With Eqs. (9), (10) and (11), the equations of the forces F_x and F_y with the three phase currents as parameters can be obtained

$$\begin{bmatrix} F_x \\ F_y \end{bmatrix} = k_{ir}\begin{bmatrix} 1 & -1/2 & -1/2 \\ 0 & \sqrt{3}/2 & -\sqrt{3}/2 \end{bmatrix} \cdot \begin{bmatrix} i_A \\ i_B \\ i_C \end{bmatrix} \quad (12)$$

D. Analysis of Nonlinearity and Cross-coupling

As can be seen from the suspension force formulas (5) and (7), the axial and both radial suspension forces are nonlinearity functions of the displacements and control currents. The Fig.4a, Fig.4b and Fig.4c are the current-force graphs of the same bearing in axial and both radial directions respectively. Effects of magnetic material saturation are not considered in these calculations. Though the graphs show that the linearity of the bearing becomes bad with a rise of the displacement and the control current, it's feasible to build the linearization mathematics models near the balance position.

At the same time, the graphs in Fig.4a and Fig.4c are perfectly symmetrical, they are fully comparable to a DC HMB [1]. So it's easier to find a stable controller for z-direction and y-direction. And the strong asymmetry in x-direction is caused by three poles geometrical asymmetrical arrangement of the radial magnetic poles about y-axis. A robust controller can handle the nonlinearity and asymmetry problems when the rotor is working in a big air gap. But if the rotor is working nearby the reference balance position, a linear controller is enough to make the bearing working well.

The asymmetry also leads to cross coupling among three-degree freedoms. Fig.4d shows the relationship among axial suspension force, x-direction and z-direction displacement. As can be seen from this 3-dimension surface, the surface becomes more bended with a rise of the axial and radial displacements. But the plane near the reference balance position shows there is little coupling as long as the displacements of the rotor is small. And as can be seen from Fig.4e, with the change of x-direction control current, there nearly isn't influence to the z-direction suspension force. Compared with Fig.3d, the influence that the radial displacements brought to the axial suspension force is much more than the radial control currents did.

Of course the cross coupling between x-direction and y-direction is also existed, but similar to the above analysis

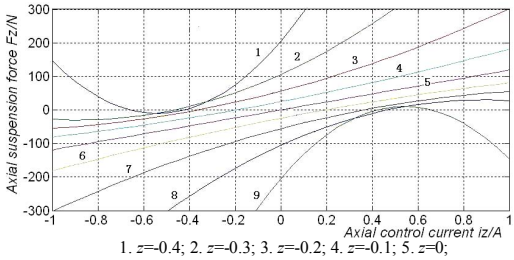

1. z=-0.4; 2. z=-0.3; 3. z=-0.2; 4. z=-0.1; 5. z=0;
6. z=0.1 ; 7. z=0.2; 8. z=0.3; 9. z=0.4

(a) Calculated current-force graph of the bearing in z-direction when x, y, i_x, i_y equal zero

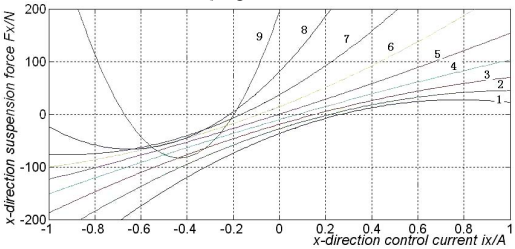

1. x=-0.4; 2. x=-0.3; 3. x=-0.2; 4. x=-0.1; 5. x=0;
6. x=0.1 ; 7. x=0.2; 8. x=0.3; 9. x=0.4

(b) Calculated current-force graph of the bearing in x-direction when z, y, i_z, i_y equal zero

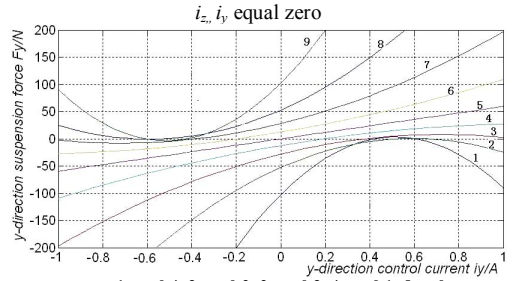

1. y=-0.4; 2. y=-0.3; 3. y=-0.2; 4. y=-0.1; 5. y=0;
6. y=0.1 ; 7. y=0.2; 8. y=0.3; 9. y=0.4

(c) Calculated current-force graph of the bearing in y-direction when x, z, i_x, i_z equal zero

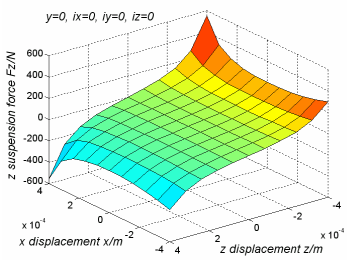

(d) Relationship among F_z ,displacement x and displacement z

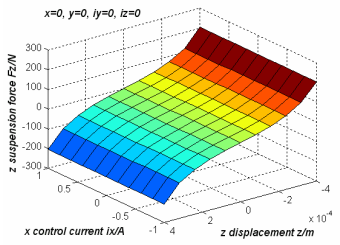

(e) Relationship among F_z, *control* current i_x and displacement z

Fig.4 Graphs of nonlinearity and cross coupling

results, all the calculated results show that nearby the reference balance position, the linearity of the magnetic bearing is ideal. So based on the linearization mathematics model as showed in Eqs.(6) and (12), it is feasible to

design a linear controller to control the bearing system well.

E. Prototype Parameter and Finite Element Analysis

A prototype is designed to support the bearingless permanent magnet synchronous motor. The design requirements and design parameters for the prototype are shown in table 1. The test bench for this prototype is as shown in Fig. 5.

TABLE I
REQUIREMENTS AND DESIGN PARAMETERS

Item	Requirements
Maximum axial resulting force F_{zmax}/ N	120
Maximum radial resulting force F_{rmax}/ N	100
Air gap length δ_0/mm	0.5
Saturation induction B_S/T	0.8
Permanent magnet material	Nd-Fe-B
Current density J_{max}/ A/mm^2	4
Axial magnetic pole area S_a/ mm^2	465
Radial magnetic pole area S_r/ mm^2	310
$(N_z i_z)_{max}$/ At	160
$(N_r i_r)_{max}$/ At	320
Outer length/ mm	39
Outer diameter/ mm	φ133

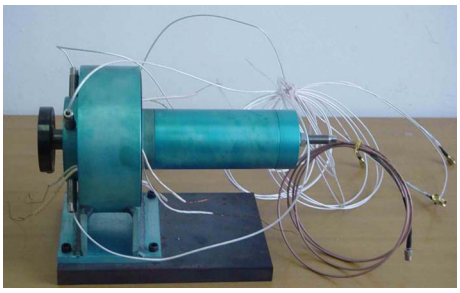

Fig.5 Test bench for AC-DC 3 degrees of freedom HMB

Based on the design parameters, a prototype model has been built in ANSYS software, which is a computer-aided engineering (CAE) software. Simulation has been conducted based on the prototype model. Fig.6a presents the permanent magnetic induction distribution in the bearing. As can be seen from the image that the magnetic fluxes are symmetrical in the radial and axial direction of the bearing, and the permanent magnetic inductions of all air gap are equal. Therefore, the simulation results are coincident with the theoretic analysis of Fig.2.

One transient working state of the prototype is simulated as shown in Fig.6b. Both the axial and the radial control coils are excited, the magnetic induction change of each air gap can be seen from the different color clouds. The incorporated fluxes of the radial or the axial gaps can generate the radial resulting force or the axial resulting force to overcome loads or disturbance forces to keep the rotor in the balance position. Results of simulation have proved that the axial and radial control flux doesn't influence each other.

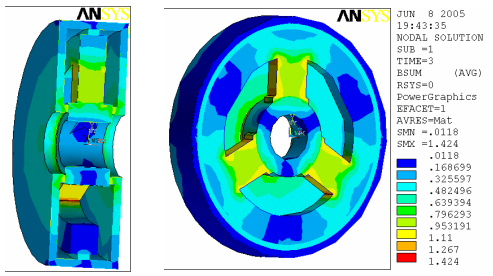

(a) Flux distribution of permanent magnet

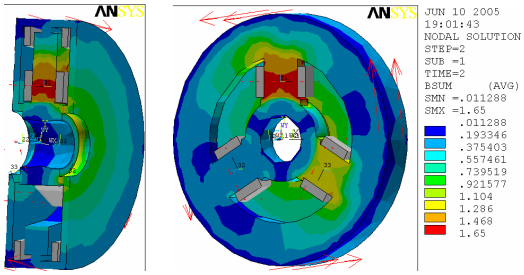

(b) Flux distribution of a transient working state

Fig.6 FEA simulation of AC-DC 3 degrees of freedom HMB

IV. DIGITAL CONTROL SYSTEM

A. Control Scheme

Equation (6) describes the relationship among axial force, the axial displacement and the axial control current. Matrix equation (12) describes the relationship between the radial forces and the radial control currents; therefore, the basic control scheme of AC-DC 3 degrees of freedom HMB is designed as is shown in Fig. 7. A hybrid circuit combined digital and analogy electronics is used to control the bearing.

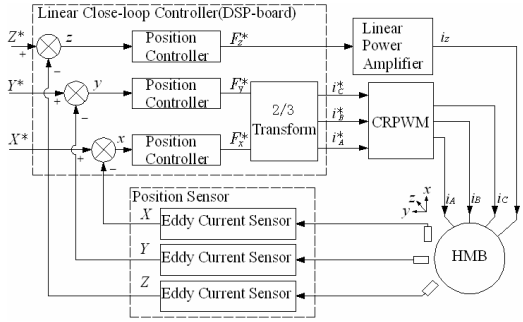

Fig. 7 Control scheme of AC-DC 3 degrees of freedom HMB

The axial displacement sensor measures the real axial position of the rotor and output the minus feedback signal to Linear Close-loop Controller (based on digital signal processor), compared with the position reference value set previously in the controller, then the controller will transform the displacement into current signal by PID method to activate the power amplifier. Lastly, the control currents provided by Linear Power Amplifier generate controllable magnetic fluxes in the axial air gaps, so the rotor can be dragged back to the balance position by the suspension force generated by the resulting magnetic flux.

Likewise, the radial displacement sensors measure the real radial position of the rotor and output minus feedback signals to Linear Close-loop Controller, compared with the position reference values set previously in the controller, and then the controller will transform the displacements into force signals by PID method. Through 2/3 transformation, 3-phase control currents signals i_A*, i_B*, and i_C* are generated, which will produce real control currents (i_A, i_B, and i_C)[5] .The control currents will generate the control flux, the suspension force will be generated by the controllable fluxes and makes the rotor suspend in the radial balance position.

B. *Hardware of Digital Control System*

The hardware of this bearing system consists of the prototype, PC, DSP-board, position sensors, interface circuits and CRPWM, etc. To realize the real time control of this digital control system, a high performance digital processor TMS320LF2407 is used in this system as a CPU, which has been used in motor control widely for it's lower cost and losses. DSP board and Power amplifier are shown in Fig.8 and Fig.9 respectively.

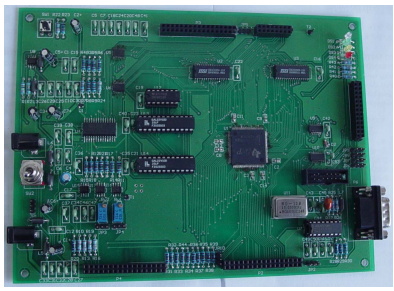

Fig.8 DSP-board for AC-DC 3 degrees of freedom HMB

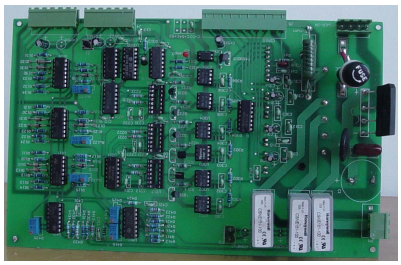

Fig.9 Power amplifier for AC-DC 3 degrees of freedom HMB

C. *Software of Digital Control System*

The software of this bearing system is constituted by a main program module and several interrupt modules. At the first, the main program finishes the configuration of Watchdog, System clock, A/D conversion and Event management, and then initializes the system variables. Finally, the main program starts the timer, opens the interrupt circulation and waiting the occurrence of interrupts. The interrupt service program module will finish the control arithmetic for the magnetic bearing's magnetic suspension forces. The program flow charts are shown in Fig.10.

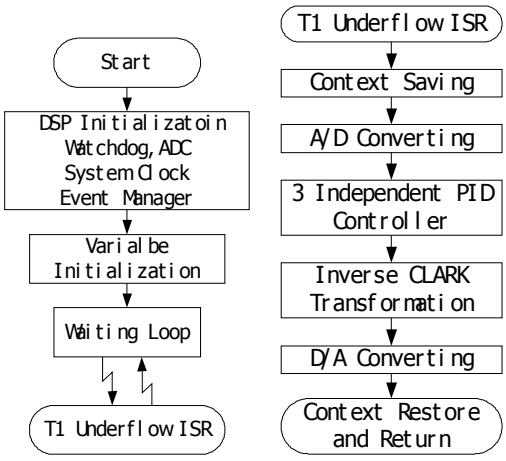

(a) Main program (b) Interrupt program

Fig.10 Program flowchart

V. CONCLUSIONS

(1) The traditional DC radial magnetic bearings are operated either by four unipolar power amplifiers or by two bipolar amplifiers, however, an AC-DC 3 degrees of freedom HMB could be driven by a 3-phase converter, which is used widely in electrical drives, so the efficiency of 3-phase converters is higher, the cost of the power amplifier is reduced.

(2) Biased flux is generated by the permanent magnet, while the control coils provide only the control flux to overcome the loads or the external disturbances. So the Ampere turns of the control coils are reduced significantly, the size and the total weight of the bearing is also reduced. Moreover, the total power consumption is reduced without the biased current, which reduces the size of the heat dissipation device too.

(3) With the characteristics of smaller size, lighter weight, lower cost, higher carrying capacity and higher efficiency, the novel AC-DC 3 degrees of freedom HMB will have wide applications in some suspending fields of special support.

REFERENCES

[1] Huangqiu Zhu, Shouqi Yuan, Bing Li, Yukun Sun, Deming Wang, and Yangguang Yan, "The working principle and parameter design for permanent magnet biased radial-axial direction magnetic bearing," *Proceedings of the CSEE*, vol. 22, no. 9, pp. 54-58, September 2002.

[2] Patrick T. McMullen, Co S. Huynh, Richard J. Hayes, "Combination radial-axial magnetic bearing," in *Proc. 7th Int. Symp. on Magnetic Bearings,* Zurich, pp. 473-478, August 2000.

[3] C. Redemann, P. Meuter, A. Ramella, T. Gempp, "30kW bearingless canned motor pump on the test bed," in *Proc. 7th Int. Symp. on Magnetic Bearings,* Zurich, pp. 189-194, August 2000.

[4] A. O. Salazar, A. Chiba, T. Fukao, "A review of developments in bearingless motors, " in *Proc. 7th Int. Symp. on Magnetic Bearings,* Zurich, pp. 335-400, August 2000.

[5] R. Schoeb, C. Redemann, T. Gempp, "Radial active magnetic bearing for operation with a 3-phase power converter," in *Proc. 4th Int. Symp. on Magnetic Suspension Technology,* Gifu, 1997